



# Spine dynamics of PSD-95-deficient neurons in the visual cortex link silent synapses to structural cortical plasticity

Rashad Yusifov<sup>a,b,c</sup>, Anja Tippmann<sup>a,c</sup>, Jochen F. Staiger<sup>b,d</sup>, Oliver M. Schlüter<sup>b,e,f,1</sup> , and Siegrid Löwel<sup>a,b,c,1,2</sup> 

<sup>a</sup>Department of Systems Neuroscience, Johann Friedrich Blumenbach Institut für Zoologie und Anthropologie, Universität Göttingen, D-37075 Göttingen, Germany; <sup>b</sup>Collaborative Research Center 889, Universität Göttingen, D-37075 Göttingen, Germany; <sup>c</sup>Campus Institute for Dynamics of Biological Networks, Universität Göttingen, D-37075 Göttingen, Germany; <sup>d</sup>Institute for Neuroanatomy, University Medical Center, Universität Göttingen, D-37075 Göttingen, Germany; <sup>e</sup>Department of Neuroscience, University of Pittsburgh, Pittsburgh, PA 15260; and <sup>f</sup>Department of Psychiatry and Psychotherapy, University Medical Center Göttingen, Universität Göttingen, D-37075 Göttingen, Germany

Edited by Michael P. Stryker, University of California San Francisco Medical Center, San Francisco, CA, and approved January 29, 2021 (received for review October 30, 2020)

**Critical periods (CPs) are time windows of heightened brain plasticity during which experience refines synaptic connections to achieve mature functionality. At glutamatergic synapses on dendritic spines of principal cortical neurons, the maturation is largely governed by postsynaptic density protein-95 (PSD-95)-dependent synaptic incorporation of  $\alpha$ -amino-3-hydroxy-5-methyl-4-isoxazolepropionic acid (AMPA) receptors into nascent AMPA-receptor silent synapses. Consequently, in mouse primary visual cortex (V1), impaired silent synapse maturation in PSD-95-deficient neurons prevents the closure of the CP for juvenile ocular dominance plasticity (jODP). A structural hallmark of jODP is increased spine elimination, induced by brief monocular deprivation (MD). However, it is unknown whether impaired silent synapse maturation facilitates spine elimination and also preserves juvenile structural plasticity. Using two-photon microscopy, we assessed spine dynamics in apical dendrites of layer 2/3 pyramidal neurons (PNs) in binocular V1 during ODP in awake adult mice. Under basal conditions, spine formation and elimination ratios were similar between PSD-95 knockout (KO) and wild-type (WT) mice. However, a brief MD affected spine dynamics only in KO mice, where MD doubled spine elimination, primarily affecting newly formed spines, and caused a net reduction in spine density similar to what has been observed during jODP in WT mice. A similar increase in spine elimination after MD occurred if PSD-95 was knocked down in single PNs of layer 2/3. Thus, structural plasticity is dictated cell autonomously by PSD-95 in vivo in awake mice. Loss of PSD-95 preserves hallmark features of spine dynamics in jODP into adulthood, revealing a functional link of PSD-95 for experience-dependent synapse maturation and stabilization during CPs.**

plasticity | silent synapses | spine dynamics | visual cortex | awake

Early life of an animal is characterized by time windows of functionally and structurally enhanced brain plasticity known as critical periods (CPs), which have been described initially in the primary visual cortex (V1) of kittens (1). During CPs, experience refines the connectivity of principal excitatory neurons to establish the mature functionality of neural networks. This refinement is governed by the constant generation and elimination of nascent synapses on dendritic spines that sample favorable connections to be consolidated and unfavorable ones to be eliminated (2–5). A fraction of nascent synapses is or becomes  $\alpha$ -amino-3-hydroxy-5-methyl-4-isoxazolepropionic acid (AMPA)-receptor silent, expressing *N*-methyl-D-aspartate (NMDA) receptors only (6–8). At eye opening, silent synapses are abundant in the primary visual cortex (V1) (9, 10) and mature during CPs by stable AMPA receptor incorporation (11–14). The pace of silent synapse maturation is governed by the opposing yet cooperative function of postsynaptic density protein of 95 kDa (PSD-95) and its paralog PSD-93, two signaling scaffolds of the postsynaptic density of excitatory synapses (12, 13). However, whether silent

synapses are preferential substrates for spine elimination during CPs remains to be investigated.

In juvenile mice (postnatal days [P] 20 to 35), a brief monocular deprivation (MD) of the dominant contralateral eye results in a shift of the ocular dominance (OD) of binocular neurons in V1 toward the open eye, mediated by a reduction of responses to visual stimulation of the deprived eye (15–17). Structurally, MD induces an increase in spine elimination in apical dendrites of layer (L) 2/3 and L5 pyramidal neurons (PNs) which is only observed during the CP and constitutes a hallmark of juvenile OD plasticity (jODP) (18–20). After CP closure, cortical plasticity declines progressively, and in standard caged-raised mice beyond P40, a 4-d MD no longer induces the functional nor anatomical changes associated with jODP (21–24).

At least three different mechanisms involved in experience-dependent maturation of cortical neural networks have been described, but the molecular and cellular mechanisms that cause CP closure remain highly debated (18, 25, 26). First, plasticity of local inhibitory neurons, such as increased inhibitory tone or a reduction of release probability by experience-dependent endocannabinoid receptor 1 (CB1R) activation was reported to close the critical

## Significance

During critical periods, restricted time windows in early brain development, cortical neural circuits get refined in an experience-dependent manner. Postsynaptic density protein-95 (PSD-95)-dependent maturation of silent glutamatergic synapses onto principal neurons is required for the termination of the critical period for ocular dominance plasticity (ODP) in the primary visual cortex (V1) of mice. Using chronic in vivo two-photon imaging of dendritic spine dynamics in V1 of awake mice, here we show that adult PSD-95-deficient neurons display increased spine elimination after a brief monocular deprivation, a structural hallmark of juvenile ODP. Thus, adult PSD-95-deficient neurons display both functional and structural hallmarks of critical period plasticity so that PSD-95-dependent silent synapse maturation and stabilization is correlated with critical period closure.

Author contributions: R.Y., O.M.S., and S.L. designed research; R.Y. performed research; A.T. and J.F.S. contributed new reagents/analytic tools; R.Y. analyzed data; and R.Y., O.M.S., and S.L. wrote the paper.

The authors declare no competing interest.

This article is a PNAS Direct Submission.

This open access article is distributed under [Creative Commons Attribution-NonCommercial-NoDerivatives License 4.0 \(CC BY-NC-ND\)](https://creativecommons.org/licenses/by-nc-nd/4.0/).

<sup>1</sup>O.M.S. and S.L. contributed equally to this work.

<sup>2</sup>To whom correspondence may be addressed. Email: sloewel@gwdg.de.

This article contains supporting information online at <https://www.pnas.org/lookup/suppl/doi:10.1073/pnas.2022701118/-DCSupplemental>.

Published March 1, 2021.

period in rodent V1 (27–29). Second, the expression of so-called “plasticity brakes,” such as extracellular matrix (ECM), Nogo receptor 1 (NgR1), paired immunoglobulin-like receptor B (PirB), and Lynx1 were correlated with the end of critical periods (30–33). Experimentally decreasing the inhibitory tone or absence of plasticity brakes enhanced ODP expression in various knockout (KO) mouse models (32, 34, 35), among which only Lynx1 KO mice were shown to exhibit functional hallmarks of jODP, such as selective deprived eye depression after a short MD (36). Structurally, Lynx1 KO mice exhibited elevated spine dynamics at baseline; however, MD induced a reduction in spine elimination in apical dendrites of L5 PNs, whereas in L2/3 PNs there was no change (37). Thus, the effects of removing plasticity brakes on structural plasticity are variable, and it remains unclear to what extent manipulating the plasticity brakes can reinstate cellular signatures of CP plasticity in the adult wild-type (WT) brain (38). Third, the progressive maturation of AMPAR-silent synapses was correlated with the closure of the CP for jODP (12, 13). Consequently, in PSD-95 KO mice, the maturation of silent synapses is impaired; their fraction remains at the eye opening level, and jODP is preserved lifelong (13). Furthermore, visual cortex-specific knockdown (KD) of PSD-95 in the adult brain reinstated jODP. In contrast, in PSD-93 KO mice, silent synapses mature precociously and the CP for jODP closes precociously (12), correlating the presence of silent synapses with functional plasticity during CPs.

While these three mechanisms of CP closure are not mutually exclusive in regulating cortical plasticity (26), it remains elusive whether CP-like structural plasticity can be expressed in the adult brain and whether silent synapses might be substrates for it. Here, we performed chronic two-photon imaging of dendrites of L2/3 pyramidal neurons in binocular V1 of PSD-95 KO (and KD) and WT mice, tracking the same dendritic spines longitudinally before, during, and after a 4-d period of MD. As previous studies have reported anesthesia effects on spine dynamics (39–41), we performed our experiments in awake mice, thoroughly trained for head fixation under the two-photon microscope. Our chronic spine imaging experiments revealed that in adult PSD-95 KO and KD mice, a brief MD indeed increased spine elimination about twofold, while adult WT mice did not display experience-dependent changes in spine elimination or spine formation. Thus, the loss of PSD-95 led to a high number of AMPAR-silent synapses which were correlated with jODP after MD, and with juvenile-like structural plasticity even in the adult brain, underscoring the importance of silent synapses for CP-timing and network maturation and stabilization.

## Results

**Four-Day MD Reduced the Spine Density in Apical Dendrites of L2/3 Pyramidal Neurons in Adult PSD-95 KO Mice.** To test the importance of AMPA-receptor silent synapses for experience-dependent structural plasticity in mouse V1, we performed chronic two-photon imaging of L2/3 pyramidal neurons before, during, and after short-term (4 d) MD in adult PSD-95 KO and WT mice. For achieving layer-specific labeling of pyramidal neurons, we electroporated in utero an eGFP (enhanced green fluorescent protein)-expressing plasmid to PSD-95 WT and KO pups at embryonic day (E) 15.5 (Fig. 1A) when L2/3 pyramidal neurons are born (*SI Appendix, Materials and Methods*).

Post hoc inspection of coronal brain slices from adult mice (>P100) confirmed that the expression of eGFP in all our experimental animals was indeed exclusive to L2/3 (Fig. 1B). Mice expressing eGFP in binocular V1 were then habituated to head fixation for chronic awake two-photon imaging (Fig. 1A and C–E). We repeatedly imaged 40 dendrites (~948  $\mu\text{m}$ ) in binocular V1 of six PSD-95 WT mice (P77 to 79; ~78), and 36 dendrites (~936  $\mu\text{m}$ ) in six KO mice (P64 to 79; ~73) with 4-d intervals during normal vision (NV), during MD and after reopening the

formerly deprived eye (RO) (Fig. 1A). A similar proportion of those dendrites in each genotype (25/5, WT: ~62% of total dendrites; 21/4, KO: ~58% of all) were also imaged with 1-d intervals, on the first days of NV and MD phases (Fig. 1A). The deprived eye was reopened immediately after imaging on day 8 (d8), and the same dendrites were imaged again 2 and 4 d thereafter.

Despite the elevated silent synapse fraction in PSD-95 KO mice (13), post hoc comparison of average spine densities ( $\pm$ SEM) during baseline imaging (d0 to d4) did not reveal significant differences between WT ( $0.846 \pm 0.021$  spine/ $\mu\text{m}$ ) and KO mice ( $0.775 \pm 0.027$  spine/ $\mu\text{m}$ ,  $P = 0.219$ ) within the linear mixed-effects model (LME), where genotype [ $F_g(1, 74) = 6.025$ ,  $P = 0.0165$ ] and time [ $F_t(1, 74) = 13.42$ ,  $P < 0.001$ ] had a significant main effect and no significant interaction [ $F_{g \times t}(4, 241) = 1.043$ ,  $P = 0.386$ ; Fig. 1F]. We then normalized the spine densities in all sessions to the respective average baseline (d0 to d4) values and compared the magnitude of relative spine density changes between and within genotypes during the 12 d of imaging (Fig. 1G). Time had a significant main effect, whereas the effect of genotype and its interaction with time was not significant [LME:  $F_g(1, 74) = 0.1216$ ,  $P = 0.7283$ ;  $F_t(4, 241) = 13.57$ ,  $P < 0.001$ ;  $F_{g \times t}(4, 241) = 1.177$ ,  $P = 0.3216$ ]. Intragroup comparison of the spine densities to the average baseline revealed a significant reduction of spine density after 4-d MD in KOs, but not in WT mice (mean  $\pm$  SEM; KO:  $-7.32 \pm 3.34\%$ ,  $P = 0.002$ ; WT:  $-3.17 \pm 2.76\%$ ,  $P = 0.200$ ), which persisted 2 d ( $-9.01 \pm 3.87\%$ ,  $P < 0.001$ ) and 4 d after RO ( $-6.78 \pm 3.73\%$ ,  $P = 0.007$ ) (Fig. 1G). Lastly, we have confirmed the effect of 4-d MD on spine density by comparing the changes in spine density ( $\Delta\text{sd}$ ) between genotypes during 4-d baseline and MD using two-way ANOVA (*SI Appendix, Fig. S1*). Here we found a significant main effect of MD and a significant interaction between MD and genotype [two-way ANOVA:  $F_g(1, 74) = 0.896$ ,  $P = 0.347$ ;  $F_{\text{md}}(1, 74) = 17.8$ ,  $P < 0.001$ ;  $F_{g \times \text{md}}(1, 74) = 6.56$ ,  $P = 0.012$ ]. The change in spine density was significantly higher in PSD-95 KO mice after 4-d MD (mean  $\pm$  SEM; post hoc comparison: KO  $-0.080 \pm 0.018$  vs. WT  $-0.026 \pm 0.012$ ,  $P = 0.021$ ).

**Doubled Spine Elimination and Reduced Spine Formation during MD in Adult PSD-95 KO Mice.** To understand the cause of the experience-dependent reduction in spine density in PSD-95 KO mice, we tracked individual spines of PSD-95 WT (Fig. 2A) and KO (Fig. 2B) dendrites during periods of normal and monocular vision.

Analyses of spine elimination ratios using generalized linear mixed-effects model (GLME) showed significant main effect of MD [ $F_{\text{md}}(1, 236) = 7.792$ ,  $P = 0.006$ ] and a significant interaction between genotype and MD [ $F_{g \times \text{md}}(1, 236) = 6.005$ ,  $P = 0.015$ ], whereas the genotype [ $F_g(1, 236) = 1.851$ ,  $P = 0.175$ ], time [ $F_t(1, 236) = 2.486$ ,  $P = 0.116$ ] or three-way interaction effects were not significant [ $F_{g \times \text{md} \times t}(3, 236) = 0.865$ ,  $P = 0.460$ ]. The following post hoc tests revealed that in WT mice, spine elimination ratios did not change significantly, after 1- (mean  $\pm$  SD; 1-d NV  $0.040 \pm 0.038$  vs. 1-d MD  $0.036 \pm 0.044$ ,  $P = 0.884$ ) or 4-d MD (4-d NV  $0.048 \pm 0.041$  vs. 4-d MD  $0.052 \pm 0.033$ ,  $P = 0.496$ ). In contrast, in KO mice, already 1-d MD increased the spine elimination ratio (Fig. 2C) from  $0.047 \pm 0.041$  during 1-d NV to  $0.064 \pm 0.040$  ( $P = 0.204$ ), and after 4-d MD there was a ~126% increase in spine elimination (Fig. 2B and D) from  $0.039 \pm 0.033$  during 4-d NV (d0 to d4) to  $0.088 \pm 0.068$  ( $P < 0.001$ ) (d4 to d8). During MD (d4 to d8), the spine elimination ratio of PSD-95 KO mice was also significantly higher compared to WT controls ( $0.052 \pm 0.033$ ,  $P = 0.017$ ) (Fig. 2D). We then confirmed these results with an additional LME analysis, comparing MD-induced changes in spine elimination ( $\Delta_E$ ) and formation ratios ( $\Delta_F$ ) between genotypes [ $F_g(1, 74) = 5.797$ ,  $P = 0.019$ ;  $F_t(1, 44) = 4.136$ ,  $P = 0.048$ ;  $F_{g \times t}(1, 44) = 1.994$ ,  $P = 0.165$ ]. While the MD-induced net change (Fig. 2E) in spine elimination ratios ( $\Delta_E$ ) for 1-d

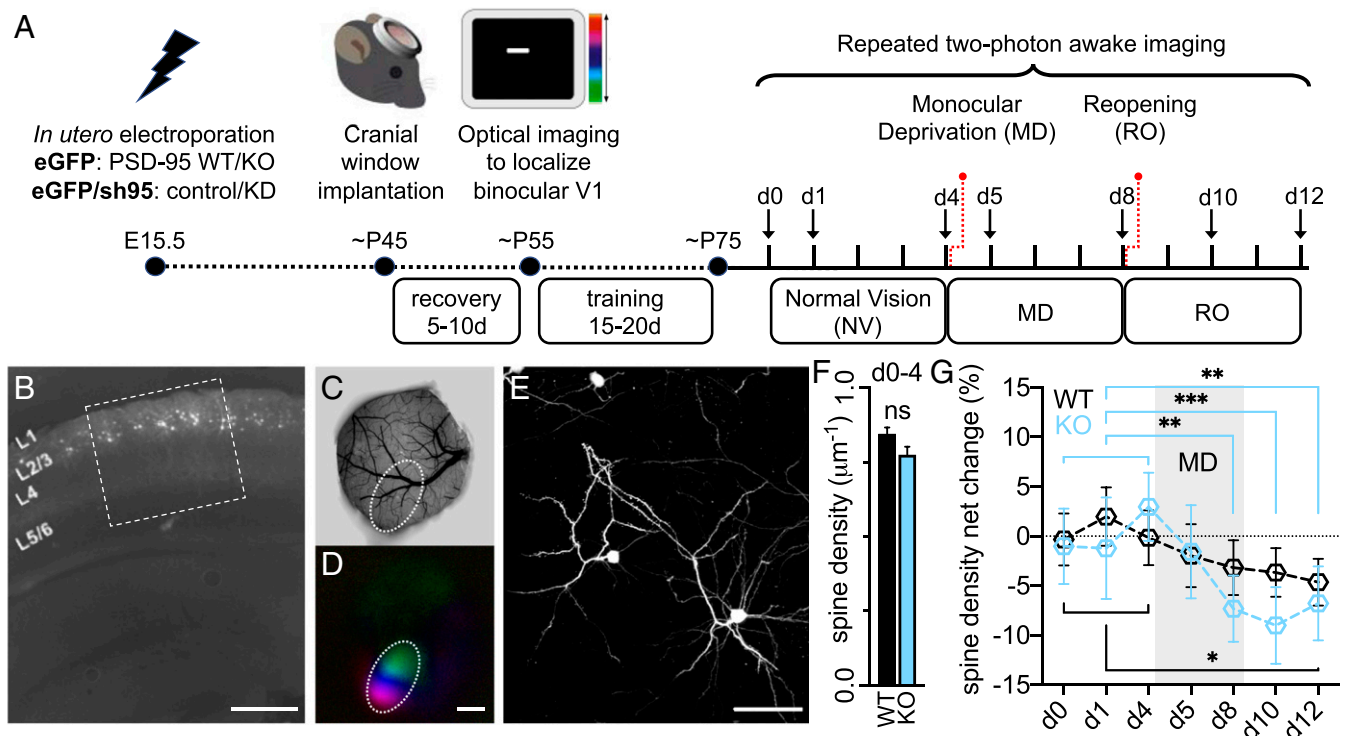


**Fig. 1.** Repeated two-photon imaging of apical dendrites of L2/3 pyramidal neurons in the primary visual cortex (V1) of awake head-fixed PSD-95 WT and KO mice during periods of normal vision (NV), monocular deprivation (MD), and after reopening the formerly deprived eye (RO). (A) Experimental timeline: a plasmid expressing eGFP or eGFP/sh95 was delivered into the left ventricle of E15.5 PSD-95 WT and KO pups and electroporated targeting V1. After implanting a chronic cranial window (~P45), optical imaging of intrinsic signals was used to locate binocular V1 at ~P50. Mice were then screened for sparse neuronal labeling and habituated to head restraint for 15 to 20 d. After baseline measurements (d0 to d4), a 4-d MD of the contralateral eye was started on d4, and the eye was reopened on d8. Awake two-photon imaging of dendritic spines was performed on all days indicated by the black arrows. (B) Coronal slice of an electroporated brain illustrating L2/3 pyramidal neuron-specific eGFP expression in V1. (Scale bar, 400  $\mu\text{m}$ .) (C) Cortical blood vessel pattern imaged through the cranial window with an outline of binocular V1 (dashed ellipse), located by (D) retinotopic mapping using intrinsic signal optical imaging (Scale bar, 1 mm). (E) Low-magnification top view of an imaged region with sparsely eGFP-labeled L2/3 pyramidal neurons. (Scale bar, 50  $\mu\text{m}$ .) (F) Average baseline spine densities ( $\pm$ SEM) of apical dendrites in PSD-95 WT and KO mice on d0 to d4. (G) The same dendrites were repeatedly imaged with 1-d (5 WT/4 KO: 25/21 dendrites) and 4-d (6 WT/6 KO: 40/36 dendrites) intervals during NV and MD periods. Imaging was continued 2 d (6 WT/6 KO: 33/31 dendrites) and 4 d (6 WT/6 KO: 33/30 dendrites) after RO. Spine density (normalized to average baseline) was significantly reduced in PSD-95 KO but not WT mice after 4-d MD, and the reduction persisted after reopening the eye. \* $P < 0.05$ ; \*\* $P < 0.01$ ; \*\*\* $P < 0.001$ ; ns,  $P > 0.05$ .

intervals was only slightly higher in KOs ( $0.017 \pm 0.011$ ) compared to WT mice ( $-0.004 \pm 0.011$ ) ( $P = 0.772$ ),  $\Delta_E$  for 4-d intervals was significantly higher in KOs ( $0.049 \pm 0.013$ ) compared to WT ( $0.004 \pm 0.008$ ,  $P = 0.004$ ) (Fig. 2E).

In WT mice, spine formation after both 1-d (1-d NV  $0.041 \pm 0.038$  vs. 1-d MD  $0.025 \pm 0.028$ ,  $P = 0.084$ ) (Fig. 2F) and 4-d MD (4-d NV  $0.048 \pm 0.039$  vs. 4-d MD  $0.037 \pm 0.032$ ,  $P = 0.125$ ) (Fig. 2G) did not change significantly [GLME:  $F_g(1, 236) = 0.052$ ,  $P = 0.820$ ;  $F_{\text{md}}(1, 236) = 12.944$ ,  $P < 0.001$ ;  $F_t(1, 236) = 9.978$ ,  $P = 0.002$ ,  $F_{g \times \text{md}}(1, 236) = 0.150$ ,  $P = 0.698$ ;  $F_{g \times \text{md} \times t}(3, 236) = 0.730$ ;  $P = 0.535$ ]. In contrast, in PSD-95 KO mice, spine formation decreased significantly after 4-d MD (NV  $0.061 \pm 0.041$  vs. MD  $0.032 \pm 0.029$ ,  $P = 0.001$ ) (Fig. 2G), while during MD, spine formation ratios were similar between WT and PSD-95 KO (Fig. 2F) (4-d MD WT:  $0.037 \pm 0.032$ ,  $P = 0.596$ ). Likewise, using LME analysis of changes in spine formation after MD [ $F_g(1, 74) = 0.325$ ,  $P = 0.570$ ;  $F_t(1, 44) = 1.30$ ,  $P = 0.260$ ;  $F_{g \times t}(1, 44) = 3.81$ ,  $P = 0.057$ ], we found that  $\Delta_F$  were comparable between WT and KO for 1-d (Fig. 2H; mean  $\pm$  SEM: WT  $-0.016 \pm 0.008$  vs. KO  $-0.012 \pm 0.009$ ,  $P > 0.9$ ) and 4-d intervals (Fig. 2H; WT  $-0.012 \pm 0.006$  vs. KO  $-0.029 \pm 0.008$ ,  $P = 0.161$ ).

In summary, a brief MD induced a decrease in spine density of L2/3 pyramidal neuron dendrites of adult PSD-95 KO but not WT mice, by doubling spine elimination and a relative reduction of spine formation compared to baseline. In contrast, MD did

not induce any significant changes in spine dynamics in adult WT mice.

**Newly Formed Spines in PSD-95 KO Mice Are More Likely to Be Eliminated during MD.** Dendritic spines with a lifetime of  $>4$  d are typically classified as persistent, while temporary spines may survive only a few days, or even hours (42). The observed strong increase in spine elimination, induced by MD in PSD-95 KO mice led us to hypothesize that in KO mice, a smaller percentage of spines present on d0 would still persist after 4-d MD. Notably, there was no genotype difference in the percentage of persistent spines (Fig. 3A) during 4-d NV (mean  $\pm$  SD, d4: WT  $90.7\% \pm 7.51$  vs. KO  $92.3\% \pm 6.28$ ) and after 4-d MD (d8: WT  $83.6\% \pm 9.40$  vs. KO  $82.1\% \pm 10.2$ , Kolmogorov–Smirnov test,  $P = 0.689$ ), suggesting that in PSD-95 KO mice, MD-induced spine elimination has preferentially targeted temporary spine populations.

We then grouped WT and KO dendrites according to the fate of newly formed spines during NV (Fig. 3B; 0.00 = all new spines were stabilized, 1.00 = all new spines were lost after MD). In fact, while in 52.5% of the WT dendrites, all of the newly formed spines were stabilized (not lost during MD), this happened in only 18.2% of KO dendrites. Furthermore, while in WT dendrites, only 9.1% of the newly formed spines were eliminated during MD, this happened in 30.3% of KO dendrites (Fig. 3B). Comparison of cumulative distributions of spine stability ratios

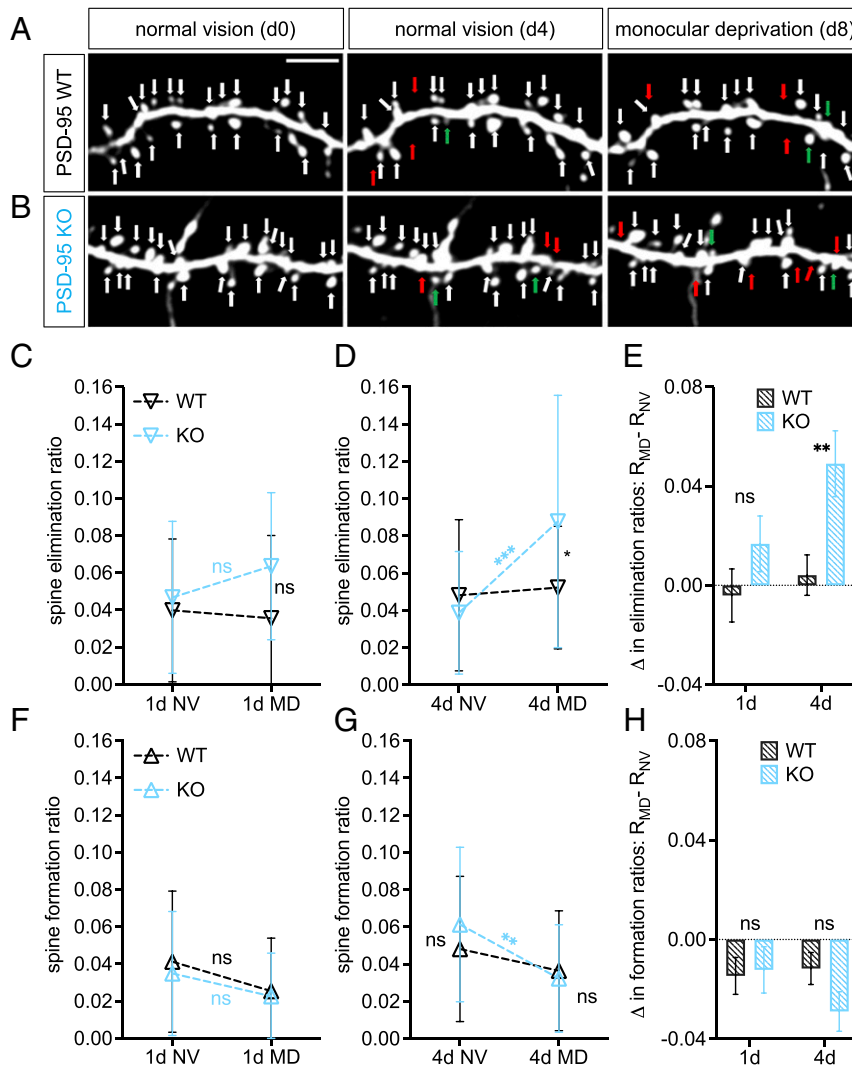


**Fig. 2.** In V1 of adult PSD-95 KO mice, monocular deprivation induces increased spine elimination and decreased spine formation on apical dendrites of L2/3 pyramidal neurons. Experience-dependent spine dynamics of L2/3 pyramidal neurons and their quantification. (A) Representative examples of dendrites from PSD-95 WT ( $n = 6$ ) and (B) KO mice ( $n = 6$ ) on d0 (Left), d4 (Middle), and d8 (Right): red arrows mark eliminated and green arrows mark newly formed spines during 4-d intervals. (Scale bar, 5  $\mu\text{m}$ ). (C and D) Mean ( $\pm$ SD) spine elimination and (F and G) spine formation ratios during 1-d (C and F; 5 WT/4 KO: 25/21 dendrites) and 4-d (D and G; 6 WT/6 KO: 40/36 dendrites) intervals, calculated as  $R = N_{\text{elim}} / (N_{\text{initial}} + N_{\text{final}})$ . (E) MD-induced change  $\Delta = R_{\text{MD}} - R_{\text{NV}}$  in spine elimination and (H) formation ratios (mean  $\pm$  SEM). \* $P < 0.05$ ; \*\* $P < 0.01$ ; \*\*\* $P < 0.001$ ; ns,  $P > 0.05$ .

thus yielded a significant difference between genotypes (Kolmogorov–Smirnov test,  $P = 0.026$ ), with a clear shift toward reduced spine stability in PSD-95 KO mice.

**Spine Dynamics in PSD-95 KO Mice Partially Normalize during Binocular Recovery.** Fast recovery of deprived eye responses after reopening of the formerly deprived eye has been suggested as another hallmark of CP plasticity in juvenile mice (18). Likewise, 2 d of reopening was sufficient to induce a recovery of ODI to pre-MD values in adult PSD-95 KO mice, whereas adult WT mice needed 4 d for ODI recovery (13). To test whether spine dynamics would also differ during recovery from MD in a mouse model with elevated fractions of AMPA-receptor silent synapses, we continued with the chronic imaging after reopening the previously deprived (contralateral) eye and compared spine dynamics in PSD-95 KO ( $n = 6$ ) and WT mice ( $n = 6$ ) 2 d (WT/KO: 33/31 dendrites) and 4 d (33/30) after reopening the MD eye (Fig. 4A and B).

GLME analysis revealed a significant main effect of visual experience [ $F_g(1, 209) = 0.590, P = 0.443$ ;  $F_v(2, 209) = 8.494, P < 0.001$ ;  $F_g \times v(2, 209) = 5.363, P = 0.005$ ]. The following post hoc comparisons showed that in WT mice, spine elimination ratios after 4-d RO (Fig. 4C) were not significantly different compared to 4-d NV ( $P = 0.075$ ) or to 4-d MD ( $P = 0.126$ ). In PSD-95 KO mice, spine elimination ratios during 4-d RO were lower ( $0.065 \pm 0.046$ ) than during MD ( $0.088 \pm 0.068, P = 0.075$ ), but still significantly elevated compared to 4-d NV ( $0.039 \pm 0.033, P = 0.009$ ) (Fig. 4C).

While spine formation also did not change in WT mice after 4-d RO [Fig. 4D; GLME:  $F_g(1, 209) = 1.954, P = 0.164$ ;  $F_v(2, 209) = 9.403, P < 0.001$ ;  $F_g \times v(2, 209) = 1.611, P = 0.202$ ] compared to NV ( $P = 0.914$ ) or MD phases ( $P = 0.268$ ), it significantly increased in PSD-95 KO mice after reopening the formerly deprived eye (4-d RO  $0.068 \pm 0.041$  vs. 4-d MD  $0.032 \pm 0.029, P < 0.001$ ), recovering to pre-MD values (Fig. 4D) (4-d NV  $0.061 \pm 0.042, P = 0.561$ ).

Two days after eye reopening, there were no differences in spine elimination [mean  $\pm$  SD; GLME:  $F_g(1, 123) = 0.306, P = 0.581$ ;

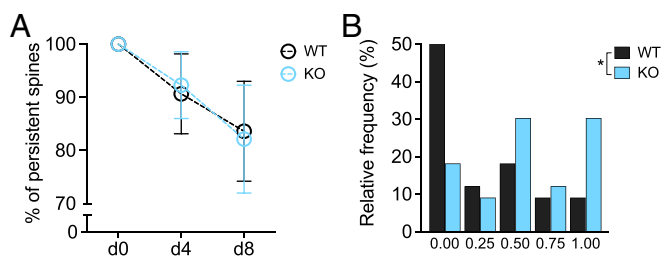


**Fig. 3.** Newly formed spines in PSD-95 KO mice are more likely to be eliminated during MD. MD-induced changes in persistent (lifetime > 4 d) and newly formed spine populations in PSD-95 KO and WT mice. (A) Percentage of persistent spines (mean  $\pm$  SD) present from d0 throughout NV and MD periods. (B) Histogram depicts relative frequency of PSD-95 WT and KO dendrites binned according to the fractions of newly formed spines that were eliminated during 4-d MD (0.00 = none eliminated; 1.00 = all new spines eliminated during MD). Note that in PSD-95 KO mice, the frequency histogram is skewed toward more spine elimination during MD.  $*P < 0.05$ .

$F_t(1, 123) = 3.052, P = 0.083; F_g \times t(1, 123) = 0.021, P = 0.885$ ; post hoc test: WT  $0.058 \pm 0.030$  vs. KO  $0.056 \pm 0.041, P = 0.583$ ] or formation ratios [mean  $\pm$  SD; GLME:  $F_g(1, 123) = 0.933, P = 0.336, F_t(1, 123) = 5.202, P = 0.024; F_g \times t(1, 123) = 1.847, P = 0.177$ ; post hoc test: WT  $0.042 \pm 0.040$  vs. KO  $0.044 \pm 0.035, P = 0.978$ ] between WT and KO mice; and 4 d after reopening, both spine elimination (WT  $0.070 \pm 0.037$  vs. KO  $0.065 \pm 0.046, P = 0.701$ ) and formation ratios were not significantly different between genotypes (Fig. 4D; WT  $0.049 \pm 0.033$  vs. KO  $0.068 \pm 0.041, P = 0.093$ ).

Overall, in adult PSD-95 KO mice, spine formation normalized to baseline values during 4-d RO, whereas spine elimination slightly decreased, but remained elevated compared to baseline (4-d NV). In contrast, in adult WT mice, neither MD nor

recovery from MD induced any significant changes in spine formation or elimination, echoing the absent functional changes (ODP).

**PSD-95 Function in Regulating Spine Stability Is Cell Autonomous.** We have previously shown that visual cortex-specific silencing of PSD-95 expression is sufficient to preserve jODP in adult WT mice, similar to our observations in adult PSD-95 KO mice (13). Here we explored whether deletion of PSD-95 in just a small subset of L2/3 pyramidal neurons in binocular V1 would cause similar experience-dependent structural changes as in the ubiquitous PSD-95 KOs. Using the same imaging protocol as for the experiments comparing spine dynamics in PSD-95 KO and WT mice, apical dendrites from eGFP-labeled L2/3 pyramidal neurons of adult WT mice (control group:  $n = 19/4$  mice,  $\sim 475 \mu\text{m}$ ; P82 to 83) or eGFP-labeled L2/3 neurons with a knockdown of PSD-95 (via sh95) in a WT environment (sh95:  $n = 21/3$  mice;  $\sim 515 \mu\text{m}$ ; P73 to 74) were repeatedly imaged with 1- and 4-d intervals during NV and MD (Fig. 5A and B).

As observed for PSD-95 KO and WT mice, average spine densities ( $\pm$ SEM) during baseline imaging (d0 to d4) were not significantly different between control ( $0.857 \pm 0.033$  spine/ $\mu\text{m}$ ) and sh95 groups [Fig. 5C;  $0.879 \pm 0.042$ ; two-way ANOVA:  $F_g(1, 38) = 0.258, P = 0.614; F_t(2, 76) = 4.63, P = 0.013; F_g \times t(2, 76) = 0.131, P = 0.877$ ; post hoc comparison:  $P > 0.9$ ].

In the control group, spine elimination after both 1 d [mean  $\pm$  SD; GLME:  $F_g(1, 152) = 1.265, P = 0.262; F_{md}(1, 152) = 1.409, P = 0.237; F_t(1, 152) = 6.767, P = 0.010; F_g \times md(1, 152) = 3.433, P = 0.066; F_g \times md \times t(3, 152) = 0.693, P = 0.558$ ; post hoc test: 1-d NV  $0.036 \pm 0.029$  vs. 1-d MD  $0.035 \pm 0.031, P > 0.9$ ; Fig. 5D] and 4-d MD (post hoc test: 4-d NV  $0.055 \pm 0.055$  vs. 4-d MD  $0.049 \pm 0.036, P = 0.586$ ) did not change significantly (Fig. 5E). After 4-d MD, similar to our observations in PSD-95 KO mice, spine

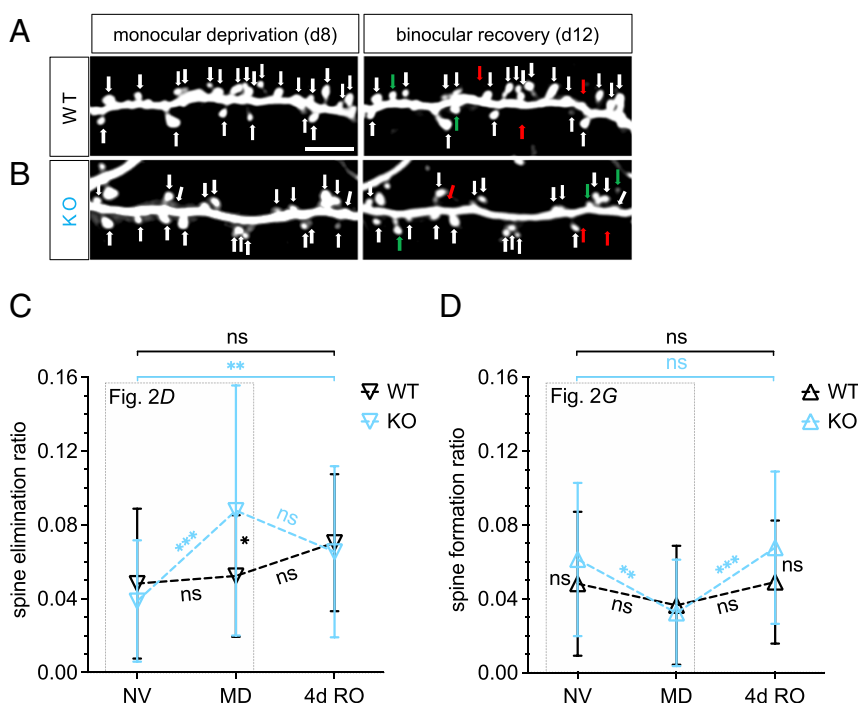


**Fig. 4.** Dendritic spine formation of L2/3 pyramidal neurons returns to baseline values in PSD-95 KO mice, while no significant changes happen in WT mice after reopening. Imaging was continued in a subset of dendrites described in Fig. 2, 4 d (6 WT/6 KO: 33/30 dendrites) after reopening the MD eye. (A) Representative examples of dendrites from PSD-95 WT and (B) PSD-95 KO mice on d8 (Left) and d12 (Right): green arrows mark formed and red arrows mark eliminated spines compared to d8 (Scale bar,  $5 \mu\text{m}$ ). (C) Comparison of mean ( $\pm$ SD) spine elimination and (D) formation ratios during 4-d reopening to NV and MD periods (gray rectangle, data replotted from Fig. 2D and G for comparison).  $*P < 0.05$ ;  $**P < 0.01$ ;  $***P < 0.001$ ; ns,  $P > 0.05$ .

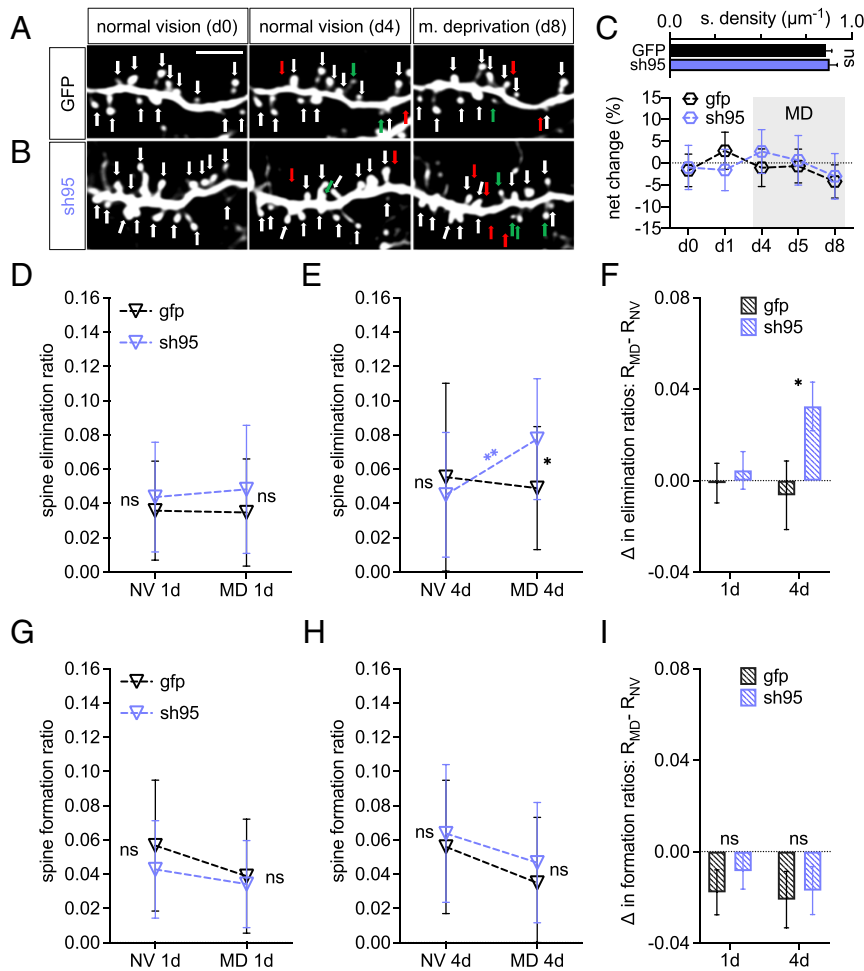


**Fig. 5.** In V1 of WT mice, MD induces increased spine elimination on apical dendrites of PSD-95 knockdown L2/3 pyramidal neurons. (A) Apical dendrites of L2/3 pyramidal neurons expressing either eGFP-tagged control (gfp; 4 mice/ $n = 19$ ) or (B) PSD-95 knockdown plasmids (sh95; 3 mice/ $n = 21$ ) were repeatedly imaged with 1- and 4-d intervals during NV and MD periods: red arrows mark eliminated, green arrows mark formed spines during 4-d intervals. (Scale bar, 5  $\mu\text{m}$ .) (C) Average baseline spine density ( $\pm$ SEM) during NV and net change of spine density during NV and MD periods (gray shaded area) relative to baseline (d0 to d4). (D and E) Mean ( $\pm$ SD) spine elimination and (G and H) spine formation ratios during (D and G) 1-d and (E and H) 4-d intervals. (F) MD-induced change ( $\Delta = R_{\text{MD}} - R_{\text{NV}}$ ) in spine elimination and (I) formation ratios (mean  $\pm$  SEM). \* $P < 0.05$ ; \*\* $P < 0.01$ ; ns,  $P > 0.05$ .

elimination ratios in sh95 dendrites also nearly doubled from  $0.045 \pm 0.036$  (4-d NV) to  $0.077 \pm 0.035$  ( $P = 0.011$ ) (Fig. 5E). Also, during MD (d4 to d8), the spine elimination ratio of sh95-expressing dendrites was significantly higher compared to controls ( $0.049 \pm 0.036$ ,  $P = 0.042$ ) (Fig. 5E). Consequently, the MD-induced change in spine elimination ( $\Delta_E$ ) in sh95-expressing dendrites after 4-d MD (Fig. 5F) [mean  $\pm$  SEM; two-way ANOVA:  $F_g(1, 38) = 2.630$ ,  $P = 0.113$ ;  $F_t(1, 38) = 2.708$ ,  $P = 0.108$ ;  $F_g \times t(1, 38) = 5.854$ ,  $P = 0.020$ ; post hoc comparison: sh95  $0.033 \pm 0.011$  vs. ctrl  $-0.006 \pm 0.015$ ;  $P = 0.027$ ], but not after 1-d MD (ctrl  $-0.001 \pm 0.009$  vs. sh95  $-0.005 \pm 0.0085$ ,  $P > 0.9$ ). Despite a significant increase in spine elimination, after 4-d MD, the reduction in spine density in sh95 dendrites relative to the baseline (d0 to d4) was nonsignificant (Fig. 5C) [mean  $\pm$  SEM;  $-3.05 \pm 5.22\%$ ; two-way ANOVA:  $F_g(1, 38) = 0.017$ ,  $P = 0.898$ ;  $F_t(2, 76) = 4.64$ ,  $P = 0.013$ ;  $F_g \times t(2, 76) = 0.139$ ,  $P = 0.870$ ; post hoc comparison:  $P = 0.358$ ].

In the control group, spine formation after 1-d [mean  $\pm$  SD; GLME:  $F_g(1, 152) = 0.004$ ,  $P > 0.9$ ;  $F_{\text{md}}(1, 152) = 10.503$ ,  $P = 0.001$ ;  $F_t(1, 152) = 1.660$ ,  $P = 0.2$ ;  $F_g \times \text{md}(1, 152) = 0.475$ ;  $P = 0.492$ ;  $F_g \times \text{md} \times t(3, 152) = 1.053$ ,  $P = 0.371$ ; post hoc comparison: 1-d NV  $0.057 \pm 0.038$  vs. 1-d MD  $0.039 \pm 0.033$ ,  $P = 0.064$ ] or 4-d MD (4-d NV  $0.056 \pm 0.039$  vs. 4-d MD  $0.035 \pm 0.038$ ,  $P = 0.068$ )

did not change significantly compared to NV (Fig. 5G and H). MD did not affect spine formation significantly in sh95-expressing dendrites either after 1-d (1-d NV  $0.043 \pm 0.028$  vs. 4-d MD  $0.034 \pm 0.025$ ,  $P = 0.260$ ) or 4-d (4-d NV  $0.064 \pm 0.040$  vs. 4-d MD  $0.047 \pm 0.035$ ,  $P = 0.154$ ). Likewise, there were also no significant differences in  $\Delta_F$  values between groups for 1-d [mean  $\pm$  SEM; two-way ANOVA: two-way ANOVA:  $F_g(1, 38) = 0.273$ ,  $P = 0.604$ ;  $F_t(1, 38) = 0.720$ ,  $P = 0.401$ ;  $F_g \times t(1, 38) = 0.150$ ,  $P = 0.701$ ; ctrl  $-0.018 \pm 0.001$  vs. sh95  $-0.009 \pm 0.008$ ,  $P > 0.9$ ] or 4-d periods (ctrl  $-0.021 \pm 0.012$  vs. sh95  $0.017 \pm 0.011$ ,  $P > 0.9$ ) (Fig. 5I).

Thus, the spine formation rate remained stable in sh95 dendrites during MD; however, similar to PSD-95 KO dendrites, spine elimination was significantly increased. These results reveal that single PSD-95-deficient neurons, surrounded by an otherwise “WT environment,” show similar structural plasticity after MD as we observed in V1 of PSD-95 KO mice. Thus, experience-dependent structural plasticity is dictated cell autonomously by PSD-95 in vivo in awake mice.

## Discussion

Critical periods are restricted time windows in development during which cortical neural networks are refined in an experience-dependent manner to achieve their mature functional properties.

We have previously shown that PSD-95-dependent maturation of AMPA-receptor silent glutamatergic synapses onto principal neurons is required for the termination of the CP for jODP in the primary visual cortex (V1) of mice (13). As increased dendritic spine elimination, induced by a brief MD, is a well-established structural hallmark of jODP (19, 20), we tested whether experience-dependent spine dynamics of L2/3 pyramidal neuron dendrites in V1 of adult (>P60) mice would also display this juvenile phenotype. This was indeed the case: by using chronic *in vivo* two-photon microscopy in awake adult mice we observed that both in PSD-95 KO mice and after visual cortex-specific knockdown of PSD-95 in WT mice, a brief MD caused a two-fold increase in dendritic spine elimination, not observed in V1 of adult WT mice before, but phenomenologically similar to the experience-dependent structural changes previously reported for jODP in WT mice during the CP (19, 20). Furthermore, the brief MD additionally caused a decrease in spine formation in PSD-95 KO mice compared to baseline measurements. In contrast, adult WT mice neither displayed modified spine elimination nor spine formation after MD. Thus, the high fraction of silent synapses in PSD-95 KO mice and “juvenile” structural cortical plasticity (after MD) are correlated. Our data thus support a model in which silent synapses serve as substrates for both functional and structural cortical plasticity with PSD-95 governing experience-dependent synapse maturation and stabilization during critical periods.

In V1 of PSD-95 KO mice, the juvenile level of ~50% AMPA-receptor silent synapses at eye opening is preserved into adulthood (13), and a visual cortex-specific knockdown of PSD-95 in adult WT mice reinstates both the juvenile level of AMPA-receptor silent synapses and jODP (12, 13). Therefore, PSD-95 is required both for synapse maturation and for closing the CP for jODP, as well as for the maintenance of the matured synaptic state. Additional correlations between silent synapses and critical period plasticity were shown with accelerated maturation and precocious CP closure by seizures in the auditory cortex (43), and dark rearing with preventing silent synapse maturation and extending jODP (12). Furthermore, the extracellular matrix glycoprotein reelin promotes silent synapse maturation, and in reelin KO mice, jODP is preserved into adulthood (44, 45). The observations of the present study expand our knowledge by showing that a high number of silent synapses in the adult brain, even in single neurons in a background of WT neurons (like in the PSD-95 knockdown experiments), is correlated with juvenile-like dendritic spine elimination after MD, a hallmark of juvenile CP structural plasticity (19, 20). These results prompt silent synapses as synaptic opportunities that are preferentially eliminated during MD and potentially also during developmental refinement if not sufficiently activated (46). This prediction is further supported by our observation that newly formed, potentially silent spines are preferentially eliminated in PSD-95-deficient neurons (Fig. 3).

While baseline spine dynamics at the apical dendrites of L2/3 pyramidal neurons was similar between adult PSD-95 WT and KO mice, a brief MD (4 d) led to a more than twofold increase (~126%) in spine elimination in adult PSD-95 KO but not WT mice, and to a ~70% increase in spine elimination in PSD-95 knockdown neurons in a WT environment. These results in PSD-95-deficient adult V1 neurons are very similar to the ~100% increase in spine elimination previously observed for L2/3 apical dendrites of juvenile (P28) WT mice after a 3-d MD (19). For L5 apical dendrites of juvenile WT mice, pronounced spine elimination (>70% increase) after a 3-d MD has also been reported (20), but so far not for adult mice beyond the critical period. It is noteworthy, that jODP after 4-d MD is mediated by a fast depression of deprived-eye responses in V1 (15, 16), potentially caused by the observed increase in spine elimination, resulting in a decrease in dendritic spine density (47). In line with previous

observations in V1 of adult WT mice (23), spine dynamics at apical dendrites of L2/3 pyramidal neurons of adult PSD-95 WT mice did not change after 4-d MD.

In contrast to juvenile mice, a prolonged MD (7 d) is needed to induce OD shifts in adult standard cage-raised WT mice. Notably, these OD shifts are mediated by a delayed enhancement of open-eye responses in V1 (21, 48), which correlate with the increased spine formation in apical dendrites of L5 pyramidal neurons observed after MD in adult mice (23). In light of the functional and anatomical studies discussed above, it is compelling to hypothesize that the reduction of deprived-eye V1 responses during jODP is caused by increased spine elimination, i.e., pruning, whereas the extended MD needed for adult ODP in standard cage-raised WT mice might promote spine formation (19, 23).

Together, our intrinsic signal optical imaging results (13) and the current findings from repeated two-photon imaging show that the experience-dependent changes of neuronal wiring and activity in adult PSD-95-deficient mice strongly resemble those repeatedly observed in juvenile CP mice (16, 19), further supporting a role of PSD-95-dependent silent synapse maturation and stabilization for CP closure. Our imaging data thus document that KO or KD of PSD-95 in V1 not only preserves jODP into adulthood, but also preserves a structural signature of critical period ODP, namely increased dendritic spine elimination after a brief visual deprivation (MD), into adulthood.

Several molecules such as chondroitin sulfate proteoglycan (CSPG), NgR1, PirB, Lynx1, and class I major histocompatibility complex (MHCI), have been described as plasticity brakes, because their genetic removal can enhance ODP in adult WT mice (30–33). Among these, Lynx1 is of particular interest because adult Lynx1 KO mice show jODP, and the structural correlates of ODP in this mouse model have been investigated *in vivo*. Genetic removal of Lynx1 increases the proteolytic activity of tissue plasminogen activator in adulthood (36), which was shown to be required for jODP expression in young mice (47, 49). In adult Lynx1 KO mice (>P60), 4-d MD induced jODP and a significant decrease in the density of thin and stubby spines, measured *in vitro*, at the distal apical dendrites of GFP-expressing L2/3 pyramidal neurons compared to the no-MD group (36). However, *in vivo* chronic imaging of spine dynamics revealed that already at baseline, both spine gain and spine elimination rates were doubled at the apical dendrites of L2/3 and L5 pyramidal neurons of Lynx1 KO compared to WT mice (37). Interestingly, 4-d MD reduced spine elimination (95% CI: 0.019 to 4.262%) in the apical dendrites of L5 PNs, whereas spine dynamics of L2/3 PNs were not significantly affected (37). Thus, albeit MD-dependent reductions in deprived-eye responses were observed in functional experiments in Lynx1 KO mice, the structural changes associated with ODP in these mice are different from what has been observed in juvenile mice.

While removal of PirB, another discussed molecule, reduced the MD duration required for expression of adult-like ODP from 8 d to 3 d, a brief (3 d) MD did not affect spine density in the apical dendrites of L5 pyramidal neurons (35). Consistent with the elevated spine density in PirB KO mice, PirB was linked to spine pruning. However, the increased functional plasticity in the PirB KO mice appear mechanistically distinct from juvenile structural plasticity (35). In the somatosensory cortex, conditional deletion of NgR1 in L5 pyramidal neurons elevated spine turnover to levels as in WT mice raised in an enriched environment (38), but whether this manipulation reinstated CP plasticity was not evaluated. Overall, none of the discussed mouse models have so far displayed the structural correlates of jODP as documented for juvenile CP mice. Thus, their role in CP plasticity versus plasticity in mature neural networks needs further analysis, as does their relation to silent synapse maturation.

In a longitudinal *in vitro* dendritic spine imaging study using hippocampal slice cultures, acute knockdown of PSD-95 was shown to increase spine turnover and impair spine stabilization after long-term potentiation (LTP) induction (50). Likewise, in an *in vivo* imaging study of apical dendrites of L2/3 pyramidal neurons in the barrel cortex of anesthetized >P40 mice, new spines that did not acquire GFP-tagged PSD-95 puncta were more likely to be lost within a day compared to spines with PSD-95 puncta (51). Consistent with these observations, our present data document that—also in the awake brain—PSD-95 is important for the stability of newly formed synapses when the neural network is challenged by a particular sensory experience (Fig. 3): our chronic imaging data show that, in PSD-95 KO but not WT mice, newly formed spines are less likely to be stabilized during MD. Instability of new spines during MD can also be an explanation for the reduced spine formation rate in PSD-95 KO mice. As *in vitro* data have indicated (52), dendritic spines can be formed and eliminated within 30 min, a time span much shorter than our imaging intervals, which could have underestimated spine formation in PSD-95 KO mice during MD.

Notably, and in contrast to hippocampal slice cultures with acute knockdown of PSD-95 (50) baseline *in vivo* spine dynamics in PSD-95-deficient neurons was not different from WT neurons, suggesting that the stabilizing effect of PSD-95 is particularly important if the input to the neural network is modified. Thus, while PSD-95 is necessary for stable AMPA-receptor insertion into the postsynaptic density of excitatory synapses during development and provides stability to spines during plasticity induction, dendritic spines might still be stabilized during baseline conditions by other membrane-associated guanylate kinases, possibly PSD-93. Moreover, even silencing PSD-95 expression sparsely in a layer-specific manner, and in just a few L2/3 neurons in an otherwise WT environment, like in the present study, caused a significant and strong increase in MD-induced spine elimination, similar to what we had observed for PSD-95 KO mice. These results thus additionally demonstrate that experience-dependent dendritic spine dynamics is regulated by PSD-95 in a cell-autonomous manner, clarifying that the increased spine elimination after MD in PSD-95-deficient neurons is not a network effect.

Despite no obvious impact on spine turnover under basal conditions in adult PSD-95 KO mice, the network functionality is compromised: both reduced silent synapse maturation as in PSD-95 KO mice and accelerated silent synapse maturation as in PSD-93 KO mice, impaired orientation discrimination (12, 13). Notably, LTP and thus synaptic AMPA-receptor incorporation are intact in PSD-95 KO mice (53–55). We hypothesize that without PSD-95, silent synapses are transiently unsilenced and contribute to refinement via the action of PSD-93. The cooperative function of the two paralogs is evident by our observation that visual perception is strongly compromised in double KO mice of PSD-93 and PSD-95 (12). Thus, the cooperative interplay of the paralogs ensures proper network maturation and functionality, while PSD-95 is essential for the stability of spines under challenging conditions, such as MD. It should be noted that both paralogs additionally engage in a multitude of interactions and potential functions in regulating synapses, including among others cell adhesion proteins, voltage gated channels, and G protein-coupled receptors (56).

In addition to displaying jODP, in adult PSD-95 KO mice, OD shifts are more transient and the ODI returns to pre-MD values already 2 d after reopening the formerly deprived eye compared to WT mice, which need 4 d for recovery (13). We were therefore interested to analyze whether the prompt ODI recovery in adult KO mice can be explained by similarly fast structural changes. In fact, in adult PSD-95 KO mice, dendritic spine formation increased and reached pre-MD (NV) baseline values 4 d after eye reopening, while in WT mice, no such changes

happened. However, spine elimination decreased slightly after RO in PSD-95 KO mice, but remained elevated (compared to pre-MD baseline) so that spine density did not yet reach pre-MD (baseline) values. Since population spine dynamics alone cannot explain the faster recovery of ODI in PSD-95 KO mice, our data suggest that synaptic plasticity mechanisms such as LTP or long-term depression (LTD) may also contribute. In fact, it is well-known that LTP is enhanced in PSD-95 KO neurons (53–55), so that in KO mice during 2-d recovery, dendritic spines receiving input from the formerly deprived eye might undergo prompt LTP, thus boosting deprived-eye responses without needing fast additional spine formation. Studies investigating spine dynamics during recovery from MD in juvenile mice, have in fact yielded mixed results: in L2/3, 2-d recovery after 6-d MD reverted MD-induced changes in spine elimination and formation back to baseline level (19); in contrast, in L5, a 3-d MD increased the spine elimination rate, which persisted even 4 d after restoration of binocular vision (20). The results suggest that MD duration may also influence how spine dynamics change after eye reopening, and more focused studies are necessary to understand the detailed structural mechanisms underlying recovery. In summary, in contrast to WT mice, we observed significant changes in spine dynamics in adult PSD-95 KO mice after reopening the previously deprived eye, but it is not yet clear whether the observed structural changes are phenotypically similar to juvenile spine dynamics during recovery from MD.

Although previous studies have investigated the role of PSD-95 for dendritic spine stability, experience-dependent spine dynamics of PSD-95-deficient neurons in the awake mouse brain have not yet been studied. Imaging dendritic spines in awake animals is important because acute exposure to various anesthetics has been documented to increase spine formation in both cortical and hippocampal neurons in young rats (39, 40) and decrease the elimination of filopodia-type dendritic protrusions *in vivo* in 1-mo-old mice (57). More importantly, a recent study has systematically investigated the effects of anesthesia on dendritic spine dynamics of CA1 pyramidal neurons after repeated exposure (41), as it is necessary for chronic imaging studies. Isoflurane, the anesthetic used in most *in vivo* imaging studies, was shown to increase spine turnover and spine density over five imaging sessions with 4-d intervals (41). Thus, in order to observe spine dynamics under physiological conditions, imaging in awake mice, as in the present study, is essential. Both our PSD-95 WT and KO mice were thoroughly habituated for head fixation under our two-photon microscope.

In conclusion, our chronic awake spine imaging data clearly demonstrate that 4-d MD leads to a drastic increase in spine elimination in PSD-95-deficient L2/3 pyramidal neurons of adult mouse V1, providing a cellular correlate for reduction of deprived-eye V1 responses in jODP. The observed structural dynamics of the dendritic spines of the L2/3 pyramidal neurons of adult PSD-95 KO/KD mice are strongly reminiscent of the experience-dependent changes that have been reported for juvenile WT mice after MD (19, 20), which notably are also characterized by a lower PSD-95 expression and higher ratios of AMPA-receptor silent synapses (9, 12–14). Our results thus emphasize the importance of PSD-95 for visual cortical synapse maturation and further consolidate the concept of silent synapse-dependent neural network stabilization during CPs.

## Materials and Methods

E15.5 PSD-95 WT and KO pups were electroporated *in utero* with a GFP-expressing plasmid to label L2/3 pyramidal neurons. At ~P45, a chronic cranial window was implanted by replacing a 4-mm diameter round piece of cranium over binocular V1 of the left hemisphere with a glass coverslip (58). At 5 to 10 d after the implantation surgery, binocular V1 was identified using intrinsic signal optical imaging (59). Mice with bright and sparse labeling of dendrites with clearly identifiable dendritic spines were proceeded

to a stepwise habituation procedure for awake head restraining under the two-photon microscope. After successful training, the same set of dendrites was imaged repeatedly for 12 d in total (Fig. 1A) during normal vision (NV: d0 to d4), after monocular deprivation (MD: d4 to d8) of the contralateral eye, and after reopening (RO: d8 to d12) the formerly deprived eye. All images were analyzed blind to both genotype and experimental condition. See *SI Appendix, Materials and Methods* for additional details.

**Data Availability.** Anonymized data have been deposited in the local university server (<https://owncloud.gwdg.de/index.php/s/H4jWiaDBLb7ksc1>) (60).

1. T. N. Wiesel, D. H. Hubel, Single-cell responses in striate cortex of kittens deprived of vision in one eye. *J. Neurophysiol.* **26**, 1003–1017 (1963).
2. Y. Zuo, A. Lin, P. Chang, W. B. Gan, Development of long-term dendritic spine stability in diverse regions of cerebral cortex. *Neuron* **46**, 181–189 (2005).
3. A. J. Holtmaat et al., Transient and persistent dendritic spines in the neocortex in vivo. *Neuron* **45**, 279–291 (2005).
4. J. T. Trachtenberg et al., Long-term in vivo imaging of experience-dependent synaptic plasticity in adult cortex. *Nature* **420**, 788–794 (2002).
5. B. Lendvai, E. A. Stern, B. Chen, K. Svoboda, Experience-dependent plasticity of dendritic spines in the developing rat barrel cortex in vivo. *Nature* **404**, 876–881 (2000).
6. J. T. Isaac, R. A. Nicoll, R. C. Malenka, Evidence for silent synapses: Implications for the expression of LTP. *Neuron* **15**, 427–434 (1995).
7. D. Liao, N. A. Hessler, R. Malinow, Activation of postsynaptically silent synapses during pairing-induced LTP in CA1 region of hippocampal slice. *Nature* **375**, 400–404 (1995).
8. M. Y. Xiao, P. Wasling, E. Hanse, B. Gustafsson, Creation of AMPA-silent synapses in the neonatal hippocampus. *Nat. Neurosci.* **7**, 236–243 (2004).
9. R. Funahashi, T. Maruyama, Y. Yoshimura, Y. Komatsu, Silent synapses persist into adulthood in layer 2/3 pyramidal neurons of visual cortex in dark-reared mice. *J. Neurophysiol.* **109**, 2064–2076 (2013).
10. S. Rumpel, G. Kattenstroth, K. Gottmann, Silent synapses in the immature visual cortex: Layer-specific developmental regulation. *J. Neurophysiol.* **91**, 1097–1101 (2004).
11. M. C. Ashby, J. T. Isaac, Maturation of a recurrent excitatory neocortical circuit by experience-dependent unsilencing of newly formed dendritic spines. *Neuron* **70**, 510–521 (2011).
12. P. D. Favaro et al., An opposing function of paralogs in balancing developmental synapse maturation. *PLoS Biol.* **16**, e2006838 (2018).
13. X. Huang et al., Progressive maturation of silent synapses governs the duration of a critical period. *Proc. Natl. Acad. Sci. U.S.A.* **112**, E3131–E3140 (2015).
14. K. S. Han, S. F. Cooke, W. Xu, Experience-dependent equilibration of AMPAR-mediated synaptic transmission during the critical period. *Cell Rep.* **18**, 892–904 (2017).
15. U. C. Dräger, Observations on monocular deprivation in mice. *J. Neurophysiol.* **41**, 28–42 (1978).
16. J. A. Gordon, M. P. Stryker, Experience-dependent plasticity of binocular responses in the primary visual cortex of the mouse. *J. Neurosci.* **16**, 3274–3286 (1996).
17. L. Mioche, W. Singer, Chronic recordings from single sites of kitten striate cortex during experience-dependent modifications of receptive-field properties. *J. Neurophysiol.* **62**, 185–197 (1989).
18. J. S. Espinosa, M. P. Stryker, Development and plasticity of the primary visual cortex. *Neuron* **75**, 230–249 (2012).
19. Y. J. Sun, J. S. Espinosa, M. S. Hoseini, M. P. Stryker, Experience-dependent structural plasticity at pre- and postsynaptic sites of layer 2/3 cells in developing visual cortex. *Proc. Natl. Acad. Sci. U.S.A.* **116**, 21812–21820 (2019).
20. Y. Zhou, B. Lai, W. B. Gan, Monocular deprivation induces dendritic spine elimination in the developing mouse visual cortex. *Sci. Rep.* **7**, 4977 (2017).
21. M. Sato, M. P. Stryker, Distinctive features of adult ocular dominance plasticity. *J. Neurosci.* **28**, 10278–10286 (2008).
22. N. B. Sawtell et al., NMDA receptor-dependent ocular dominance plasticity in adult visual cortex. *Neuron* **38**, 977–985 (2003).
23. S. B. Hofer, T. D. Mrsic-Flogel, T. Bonhoeffer, M. Hübener, Experience leaves a lasting structural trace in cortical circuits. *Nature* **457**, 313–317 (2009).
24. K. Lehmann, S. Löwel, Age-dependent ocular dominance plasticity in adult mice. *PLoS One* **3**, e3120 (2008).
25. T. K. Hensch, E. M. Quinlan, Critical periods in amblyopia. *Vis. Neurosci.* **35**, E014 (2018).
26. W. Xu, S. Löwel, O. M. Schlüter, Silent synapse-based mechanisms of critical period plasticity. *Front. Cell. Neurosci.* **14**, 213 (2020).
27. B. Jiang et al., The maturation of GABAergic transmission in visual cortex requires endocannabinoid-mediated LTD of inhibitory inputs during a critical period. *Neuron* **66**, 248–259 (2010).
28. S. J. Kuhlman et al., A disinhibitory microcircuit initiates critical-period plasticity in the visual cortex. *Nature* **501**, 543–546 (2013).
29. H. J. Luhmann, D. A. Prince, Postnatal maturation of the GABAergic system in rat neocortex. *J. Neurophysiol.* **65**, 247–263 (1991).
30. J. Syken, T. Grandpre, P. O. Kanold, C. J. Shatz, PirB restricts ocular-dominance plasticity in visual cortex. *Science* **313**, 1795–1800 (2006).
31. H. Morishita, J. M. Miwa, N. Heintz, T. K. Hensch, Lynx1, a cholinergic brake, limits plasticity in adult visual cortex. *Science* **330**, 1238–1240 (2010).
32. A. W. McGee, Y. Yang, Q. S. Fischer, N. W. Daw, S. M. Strittmatter, Experience-driven plasticity of visual cortex limited by myelin and Nogo receptor. *Science* **309**, 2222–2226 (2005).
33. T. Pizzorusso et al., Reactivation of ocular dominance plasticity in the adult visual cortex. *Science* **298**, 1248–1251 (2002).
34. A. Harauzov et al., Reducing intracortical inhibition in the adult visual cortex promotes ocular dominance plasticity. *J. Neurosci.* **30**, 361–371 (2010).
35. M. Djurisic et al., PirB regulates a structural substrate for cortical plasticity. *Proc. Natl. Acad. Sci. U.S.A.* **110**, 20771–20776 (2013).
36. N. Bukhari et al., Unmasking proteolytic activity for adult visual cortex plasticity by the removal of Lynx1. *J. Neurosci.* **35**, 12693–12702 (2015).
37. M. Sajo, G. Ellis-Davies, H. Morishita, Lynx1 limits dendritic spine turnover in the adult visual cortex. *J. Neurosci.* **36**, 9472–9478 (2016).
38. F. V. Akbik, S. M. Bhagat, P. R. Patel, W. B. Cafferty, S. M. Strittmatter, Anatomical plasticity of adult brain is titrated by Nogo Receptor 1. *Neuron* **77**, 859–866 (2013).
39. A. Briner et al., Volatile anesthetics rapidly increase dendritic spine density in the rat medial prefrontal cortex during synaptogenesis. *Anesthesiology* **112**, 546–556 (2010).
40. S. Kaech, H. Brinkhaus, A. Matus, Volatile anesthetics block actin-based motility in dendritic spines. *Proc. Natl. Acad. Sci. U.S.A.* **96**, 10433–10437 (1999).
41. W. Yang et al., Anesthetics uniquely decorrelate hippocampal network activity, alter spine dynamics and affect memory consolidation. *bioRxiv*: 10.1101/2020.06.05.135905 (2020).
42. K. P. Berry, E. Nedivi, Spine dynamics: Are they all the same? *Neuron* **96**, 43–55 (2017).
43. H. Sun et al., Early seizures prematurely unsilence auditory synapses to disrupt thalamocortical critical period plasticity. *Cell Rep.* **23**, 2533–2540 (2018).
44. J. Pielecka-Fortuna et al., The disorganized visual cortex in reelin-deficient mice is functional and allows for enhanced plasticity. *Brain Struct. Funct.* **220**, 3449–3467 (2015).
45. S. Qiu, E. J. Weeber, Reelin signaling facilitates maturation of CA1 glutamatergic synapses. *J. Neurophysiol.* **97**, 2312–2321 (2007).
46. W. J. Bian, W. Y. Miao, S. J. He, Z. Qiu, X. Yu, Coordinated spine pruning and maturation mediated by inter-spine competition for cadherin/catenin complexes. *Cell* **162**, 808–822 (2015).
47. N. Mataga, Y. Mizuguchi, T. K. Hensch, Experience-dependent pruning of dendritic spines in visual cortex by tissue plasminogen activator. *Neuron* **44**, 1031–1041 (2004).
48. M. Y. Frenkel et al., Instructive effect of visual experience in mouse visual cortex. *Neuron* **51**, 339–349 (2006).
49. N. Mataga, N. Nagai, T. K. Hensch, Permissive proteolytic activity for visual cortical plasticity. *Proc. Natl. Acad. Sci. U.S.A.* **99**, 7717–7721 (2002).
50. I. Ehrlich, M. Klein, S. Rumpel, R. Malinow, PSD-95 is required for activity-driven synapse stabilization. *Proc. Natl. Acad. Sci. U.S.A.* **104**, 4176–4181 (2007).
51. M. Cane, B. Maco, G. Knott, A. Holtmaat, The relationship between PSD-95 clustering and spine stability in vivo. *J. Neurosci.* **34**, 2075–2086 (2014).
52. F. Engert, T. Bonhoeffer, Dendritic spine changes associated with hippocampal long-term synaptic plasticity. *Nature* **399**, 66–70 (1999).
53. M. Migaud et al., Enhanced long-term potentiation and impaired learning in mice with mutant postsynaptic density-95 protein. *Nature* **396**, 433–439 (1998).
54. J. C. Béique et al., Synapse-specific regulation of AMPA receptor function by PSD-95. *Proc. Natl. Acad. Sci. U.S.A.* **103**, 19535–19540 (2006).
55. H. J. Carlisle, A. E. Fink, S. G. Grant, T. J. O'Dell, Opposing effects of PSD-93 and PSD-95 on long-term potentiation and spike timing-dependent plasticity. *J. Physiol.* **586**, 5885–5900 (2008).
56. M. Sheng, M. J. Kim, Postsynaptic signaling and plasticity mechanisms. *Science* **298**, 776–780 (2002).
57. G. Yang, P. C. Chang, A. Bekker, T. J. Blanck, W. B. Gan, Transient effects of anesthetics on dendritic spines and filopodia in the living mouse cortex. *Anesthesiology* **115**, 718–726 (2011).
58. B. Joachimsthaler, D. Brugger, A. Skodras, C. Schwarz, Spine loss in primary somatosensory cortex during trace eyeblink conditioning. *J. Neurosci.* **35**, 3772–3781 (2015).
59. V. A. Kalatsky, M. P. Stryker, New paradigm for optical imaging: Temporally encoded maps of intrinsic signal. *Neuron* **38**, 529–545 (2003).
60. R. Yusifov, Spine\_data. GWDG. <https://owncloud.gwdg.de/index.php/s/H4jWiaDBLb7ksc1>. Deposited 17 February 2021.